2013 European Control Conference (ECC)
July 17-19, 2013, Zürich, Switzerland.

Modeling and Online-Identification of Electrically Stimulated Antagonistic Muscles for Horizontal Shoulder Abduction and Adduction

P. Spagnol[1], C. Klauer[2], F Previdi[3], J. Raisch[2,4] and T. Schauer[2]

Abstract— **A comparison of two different models of a pair of antagonistic muscles for horizontal shoulder abduction and adduction is presented. The proposed models are based on the so called Hill-model: a mechanical framework (inertia, dampers and springs) is used for their development. The models consider as inputs the estimates of the activation states of the muscles based on digital filtering of the evoked electromyogram (eEMG). Model outputs are angular velocity and position. Both models show good results in terms of performance, but they are different in terms of number of parameters that need to be identified and in terms of physical interpretation. One of the models, in fact, describes the muscle as a spring that generates torque by changing its stiffness parameter depending on its activation level. In order to enable adaptive model-based feed-forward and feedback control strategies for angular position/velocity control, an online-identification method based on an Extended Kalman Filter (EKF) is introduced for one of the two models. Simulation and experimental results show the good performance in terms of convergence time and accuracy of the estimation.**

I. INTRODUCTION

Paralyzed or paretic muscles can be made to contract by applying electrical currents to the intact peripheral motor nerves innervating them. When the electrically elicited muscle contractions are coordinated in a manner that provides function, the technique is called functional electrical stimulation (FES). FES is also often used for rehabilitation purposes or in neuro-prosthesis for restoring lost motor functions. The electrical pulses are applied through electrodes attached to the skin or implanted electrodes. The resulting movement of an applied stimulation pattern is difficult to be predicted due to the variability among different patients and for the same patient due to different physical conditions, such as fatigue and the positioning of the electrodes every rehabilitation session. Commonly, model-based feed-forward and feedback control strategies are used in order to generate defined motion trajectories [1]. To design controllers for FES systems it can be useful to have accurate models which describe the relation between the stimulation parameters and the resulting force, moment or movement. Moreover, the possibility of identifying online model parameters for different patients and conditions is useful for calibrating controllers or designing adaptive ones (see [2], [3] and [4])

Several studies has been accomplished in the past in order to describe and predict tension, based on some input stimulation [5]. The majority of the developed models are based on modified Hill-type muscle models that describe the force/torque produced by a muscle as a function of stimulation activity and both muscle length and velocity [6] (see Fig. 1).

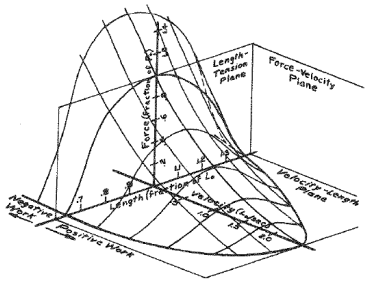

Fig. 1 - Three dimensional plot showing contractile element force as a function of length and velocity of the muscle for a specific activation level.

In this paper the interest is on controlling a human joint by the stimulation of a corresponding pair of antagonistic muscles. Important movements influenced by antagonistic muscles are e.g. the elbow extension/flexion or the horizontal shoulder abduction/adduction. The latter will be considered in detail within this contribution.

One of the most important components of muscle modeling is the nonlinear recruitment curve which describes the number of motor units activated by FES. In a previous work [7], a way to estimate the amount of recruited motor units (lambda) due to the stimulation pulse has been described. Moreover, a way to use the evoked Electromyogram (eEMG) to linearize the motor unit recruitment by feedback has been proposed. The controller (named λ-Controller) automatically adjusts the stimulation intensity according to the measured muscle recruitment state. Filtering the estimated recruitment state through a known 2nd order calcium dynamics of the muscle yields the activation state of the muscle. Thus, it is possible to consider this estimated activation state as the input of the muscle system that has to be identified. In this way it is possible to directly refer to a Hill-type model ([8] and [6]) to build up an antagonistic muscle model.

In this paper two models are investigated that are based on simple mechanical elements (inertia, springs and dampers). Both models are compared in terms of number of parameters and performance. Moreover, for one of the two models, which explains the muscle as a variable spring, an on-line identification approach based on Extended Kalman Filter (EKF) is outlined.

[1]Dipartimento di Elettronica e Informazione, Politecnico di Milano, Milano, Italy spagnol@elet.polimi.it
[2]Control Systems Group, Technische Universität Berlin, Germany
[3]Dipartimento di Ingegneria, Universit di Bergamo Dalmine (BG), Italy
[4]Systems and Control Theory Group, Max Planck Institute for Dynamics of Complex Technical Systems,Magdeburg, Germany

In Section II the experimental set-up and the λ-Controller are presented. The proposed models and the experimental data used for identification are described in detail in Section III. In the same section the off-line identification results are presented and finally the models are compared. In Section IV it is shown how to estimate on-line the parameters of one model based on an EKF.

II. EXPERIMENTAL SETUP AND RECRUITMENT CONTROL

A. Experimental Set-up

The used set-up is shown in Fig. 2 and consists of an passive exoskeleton (ARMEO, Hocoma AG, Switzerland) for weight compensation with angle sensors, a stimulation system (REHASTIM, Hasomed GmbH, Germany), a 24-bit EMG-amplifier (PHYSIOSENSE, developed at TU Berlin), an inertial motion unit (IMU) (RAZORIMU 9DOF, Sparkfun, United Kingdom) and a PC running Linux with RT-Preemption-Patch. All devices are connected to the PC through USB interfaces.

The subject's arm is placed inside the exoskeleton as shown and the arm movement is limited to horizontal shoulder abduction and adduction. The corresponding angle ϑ is defined as shown in Fig. 2 whereas $\vartheta = 0$ describes the rest position of the arm. This angle and its first time derivative are determined by fusing the outputs of the exoskeleton angle sensors and the IMU information. Data from experiments with one healthy subject have been recorded.

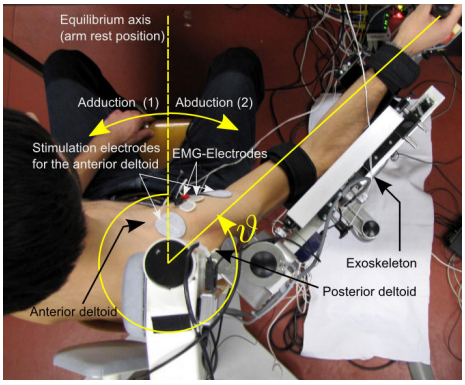

Fig. 2 - Experimental Set-up.

Current-controlled stimulation impulses are applied through self-adhesive hyrdo-gel electrodes at a stimulation frequency of 25 Hz. The anterior part of the deltoid muscle is stimulated to cause horizontal shoulder adduction. Horizontal abduction is produced by stimulation of the posterior part of the deltoid muscle. Signals related to adduction and abduction will be denoted by the indices 1 and 2 respectively. For EMG measurement at the stimulated muscles, smaller AgCl electrodes are placed between each pair of stimulations electrodes. The FES evoked EMG (eEMG) is recorded at a sampling rate of 4kHz.

For both muscles, the eEMG is filtered as described in [7] to estimate the states $\lambda_i, \quad i = 1,2$, of muscle recruitment.

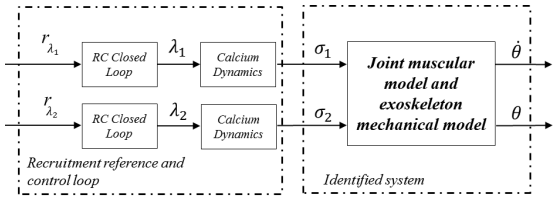

Fig. 3 - Scheme for collecting data for model identification.

Two λ-controllers, also introduced in [7], automatically adjust the stimulation intensity (pulse charge) in order to generate the desired recruitment levels $r_{\lambda_i}, \quad i = 1,2$.

The open source real-time dynamic block simulation system OPENRTDYNAMICS (http://openrtdynamics.sf.net) is used for implementation of all time critical components and provides a network communication to a QT4-GUI. The design of the control system is carried out with help of the program system SCILAB (http://www.scilab.org).

III. MODELING AND OFF-LINE IDENTIFICATION

In this section, at first the definition of inputs and outputs is given. Then two models are presented: both are able to include the Hill-type model description outlined in the introduction.

Model inputs are the activation levels of each stimulated muscle (cf Fig. 3). The activation level σ_i ($\sigma_i \geq 0$) of the muscle i is obtained by feeding the recruitment state λ_i (available from EMG measurements) through a 2nd order calcium dynamics that is taken from literature [9]. Model outputs are $\dot{\theta}$ and θ, the angular speed and position.

A. Design of experiments for model identification

In order to evaluate the fitting performance of the models an identification reference test is needed. This test consists on pseudo-random steps of r_{λ_1} and r_{λ_2}. Steps are not simultaneously applied to both muscles - i.e. when one muscle is stimulated the other is relaxed. The recruitment states λ_1 and λ_2 and the response in terms of position and speed are shown in Fig. 4. As one can see in Fig. 4, due to stick and slip behavior of the system at slow speed, the

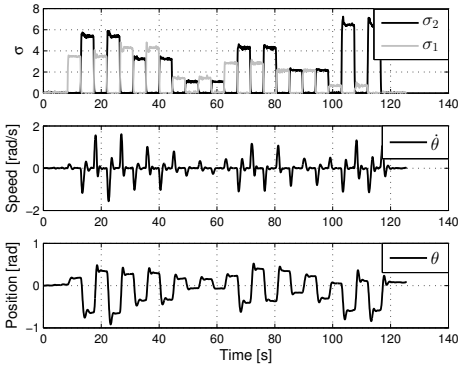

Fig. 4 - Reference test for identification. The first plot shows the muscle activation levels when using λ-control for the muscle recruitment state. Angular velocity and position are shown in the other two subplots.

equilibrium position (that corresponds to $\theta = 0$) is not always reached again at the end of the experiment. The used model structure uses a very simple friction model that does not capture such effects completely. For this reason, the applied non-linear least squares identification method takes measured and simulated angular velocities into account instead of the angular positions. The value of the velocity at equilibrium is always equal to zero. The performance index used to evaluate the model accuracy is the normalized squared L2-norm of the angular velocity (and position) fitting error. In (1) is shown how to calculate the index in the case of angular velocity:

$$J_{L_2{}^2}(\hat{\dot{\theta}}) = \frac{\frac{1}{N}\sum_{k=1}^{N}\left(\dot{\theta}(k) - \hat{\dot{\theta}}(k)\right)^2}{\frac{1}{N}\sum_{k=1}^{N}\left(\dot{\theta}(k) - \left(\frac{1}{N}\sum_{i=1}^{N}\dot{\theta}(i)\right)\right)^2} \qquad (1)$$

Values of $J_{L_2{}^2}$ near to zero indicate a good fitting performance of the model. $\hat{\dot{\theta}}$ is the angular velocity from simulation and N is the total number of samples of the experiment.

B. Model with active torque due to stimulation

The first model considered is based on an active part that depends linearly on the muscle activation state and a passive part that is composed by a constant spring and damper as well as two variable springs and dampers (function of σ_1 and σ_2). The equation that describes the model is:

$$\begin{aligned}\alpha\Big(a_1\sigma_1 + a_2\sigma_2\Big) = \alpha\Big(J\ddot{\theta} + R_m\dot{\theta} + K_m\theta + f_s(\dot{\theta}) + \cdots \\ + K_1\sigma_1\theta + K_2\sigma_2\theta + R_1\sigma_1\dot{\theta} + R_2\sigma_2\dot{\theta}\Big)\end{aligned} \qquad (2)$$

where J [kg m^2] is the rotational inertia of the arm and the exoskeleton, R_m [kg m^2/s] is the damping coefficient due to the mechanical properties of the exoskeleton and K_m [kg m^2/s^2] is the stiffness coefficient due to the mechanical properties of the exoskeleton. $f_s(\dot{\theta}) = c\,\mathrm{sign}(\dot{\theta})$ [Nm] is the static friction function with a positive constant c that has been determined from simple pendulum tests.

K_1 and K_2 [kg m^2/s^2] are the stiffness coefficients that influence the variable elastic forces; in fact these forces are suppose to be linearly dependent to σ_1 and σ_2. R_1 and R_2 [kg m^2/s] are the damping coefficients that influence the variable viscous forces; as the elastic forces, viscous forces are supposed to be linearly dependent on σ_1 and σ_2. Finally the active part of the system is characterized by the two torque coefficient a_1 and a_2 [Nm]. Produced torque by the antagonistic muscles is proportional to their activation level. As one can see in equation (2), the coefficient α multiplies all the terms. This implies that, for instance, it is possible to fix the value of αJ to a certain value and then identify the model that is normalized by this choice. During the identification process, it has been considered $\alpha J = 1$. The ($\tilde{}$) indicates normalized coefficients of the model. A comparison between measured and simulated angular velocities and positions is shown in Fig. 5. Table I shows the identified parameters and the model performance indices. A validation data set made up by increasing steps of r_{λ_1} and r_{λ_2} has been used.

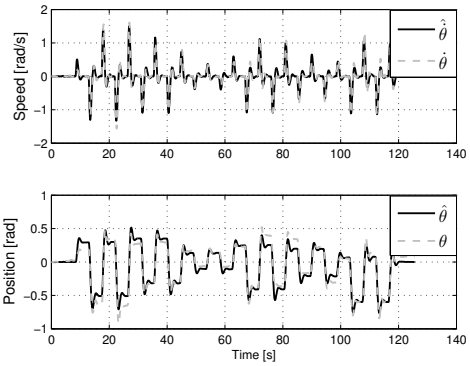

Fig. 5 - Identification results for the first model.

TABLE I
PARAMETERS AND PERFORMANCE INDICES OF THE FIRST MODEL.

(a)

Identification Result	
Parameter	Value
$\tilde{a}_1$ $[rad\ s^{-2}]$	-0.77
$\tilde{a}_2$ $[rad\ s^{-2}]$	0.76
$\tilde{K}_1$ $[s^{-2}]$	2.33
$\tilde{K}_2$ $[s^{-2}]$	0.62
$\tilde{R}_1$ $[s^{-1}]$	0.89
$\tilde{R}_2$ $[s^{-1}]$	0.43
$\tilde{K}_m$ $[s^{-2}]$	7.40
$\tilde{R}_m$ $[s^{-1}]$	1.95
$\tilde{c}$ $[rad\ s^{-1}]$	0.04
$\tilde{J}$ $[adim]$	1

(b)

Performance indices	
Index	Value
$J_{L_2{}^2}(\hat{\dot{\theta}})$	7.39%
$J_{L_2{}^2}(\hat{\theta})$	5.74%

Fig. 6 shows the comparison between $\hat{\dot{\theta}}(t)$ and $\dot{\theta}(t)$ and between $\hat{\theta}(t)$ and $\theta(t)$. In this case performance index are $J_{L_2{}^2}(\hat{\dot{\theta}}) = 13.8\%$ and $J_{L_2{}^2}(\hat{\theta}) = 15.0\%$ respectively.

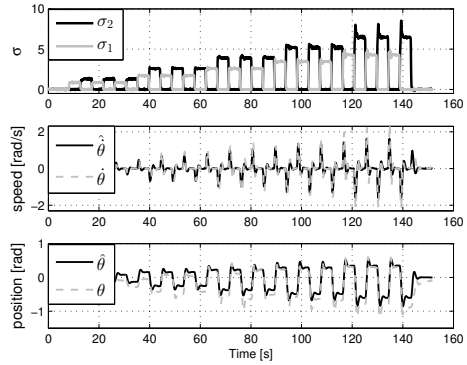

Fig. 6 - Validation results for the first model.

C. Model with variable damping and stiffness

The second investigated model structure considers a single muscle as a variable spring that is able to generate and modulate torque by changing its stiffness and damping coefficient. In some studies, [10], [11] and [12], it has been shown that a voluntarily contracting muscle with intact reflexes shows a linear relationship between its stiffness and the generated

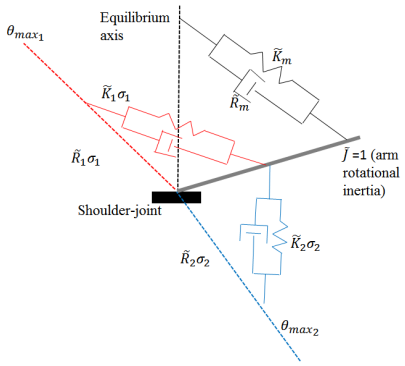

Fig. 7 - Scheme of the second proposed model: notice that the torque is generated thanks to the increased muscular stiffness

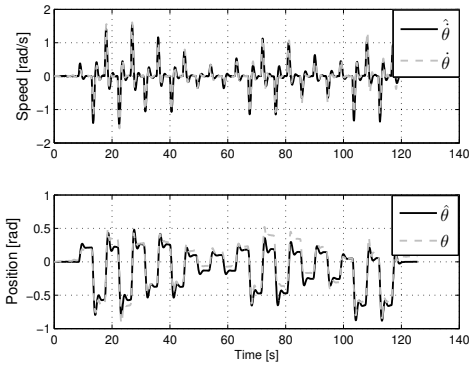

Fig. 8 - Identification results for the second model.

force. In this paper is postulated that the force generated by the muscle is proportional to a spring stiffness, that varies linearly depending on the value of σ_1 and σ_2. The equation that describes the model is:

$$\begin{aligned}&\alpha\Big(K_1\sigma_1(\theta_{max_1}-\theta)+K_2\sigma_2(\theta_{max_2}-\theta)\Big)=\\&\alpha\Big(R_1\sigma_1\dot{\theta}+R_2\sigma_2\dot{\theta}+J\ddot{\theta}+R_m\dot{\theta}+K_m\theta+f_s(\dot{\theta})\Big)\end{aligned}\tag{3}$$

where $\theta_{max_1}=\frac{5}{6}\pi$ and $\theta_{max_2}=-\frac{\pi}{3}$ are the maximum reachable angles. Also in this case, the tilde symbol ($\tilde{}$) indicates normalized model parameters, assuming $\alpha J=1$. A graphic representation of the second model structure is depicted in Fig. 7. In comparison to the model (2), this model generates the torque as the result of increasing muscle stiffness that depends on the muscle contraction (i.e. the muscle activation state) and its spatial position and speed. Fig. 8 shows the comparison between measured data and simulated one for identification data set. Estimated model parameters and the model performance indices are shown in Table II. It should be noticed in Table II that two parameters of the model, $\tilde{R}_1$ and $\tilde{R}_2$, become zero . Therefore the model can be further simplified. In the case of validation data set the performance indices are $J_{L_2{}^2}(\hat{\theta})=12.02\%$ and $J_{L_2{}^2}(\hat{\theta})=12.00\%$.

D. Comparison

The models presented in subsections III-B and III-C are very similar in terms of fitting performance. However, in terms of interpretation and number of parameters that needs to be identified, the models are completely different. The first model needs nine parameters to be identified, while the second needs just five. Moreover, the second model gives a particular description of how the torque is generated by muscles: the muscle stiffness is proportional to the activation level and the torque generated depends on the spatial position of the arm. Comparing this model with the three-dimensional representation of the Hill-type model shown in Fig. 1, one can see, that each of the two antagonistic muscle is modeled as a linearization of the surface section shown in Fig. 1 characterized by positive velocity (positive work of the muscle) and normalized muscle length < 1 (so muscular contraction from its rest length). Finally, the second model is more suitable to be identified in a on-line process because it is characterized by less parameters - without penalizing signals fitting. For this reason the online estimation presented next will be based on it.

TABLE II

PARAMETERS AND PERF. INDICES OF THE SECOND MODEL.

(a)

Identification Results	
Parameter	Value
$\tilde{K}_1\ [s^{-2}]$	0.49
$\tilde{K}_2\ [s^{-2}]$	0.33
$\tilde{R}_1\ [s^{-1}]$	0.00
$\tilde{R}_2\ [s^{-1}]$	0.00
$\tilde{K}_m\ [s^{-2}]$	6.56
$\tilde{R}_m\ [s^{-1}]$	2.43
$\tilde{c}\ [rad\ s^{-2}]$	0.04
$\tilde{J}\ [adim]$	1

(b)

Performance indices	
Index	Value
$J_{L_2{}^2}(\hat{\theta})$	6.83%
$J_{L_2{}^2}(\hat{\theta})$	7.15%

IV. ONLINE IDENTIFICATION

In order to enable adaptive control strategies like self-tuning control an online identification approach based on an Extended Kalman Filter (EKF) is presented in this section. The approach is based on the second model described by Eq. (3). An online identification can track slowly changing system parameters e.g. due to muscular fatigue, changing reflexes etc.

A. Extended Kalman Filter

The dynamic model (3) can be discretized in time and compactly written as state-space model with the following state, input and output vectors:

$$\begin{aligned}\mathbf{x}&=\begin{bmatrix}\theta & \dot{\theta} & \tilde{K}_1 & \tilde{K}_2 & \tilde{R}_m & \tilde{K}_m\end{bmatrix}'\\&=\begin{bmatrix}x_1 & x_2 & x_3 & x_4 & x_5 & x_6\end{bmatrix}'\end{aligned}\tag{4}$$

$$\mathbf{y}=\begin{bmatrix}\theta & \dot{\theta}\end{bmatrix}'=\begin{bmatrix}y_1 & y_2\end{bmatrix}'\tag{5}$$

$$\mathbf{u}=\begin{bmatrix}\sigma_1 & \sigma_2 & f_s(\dot{\theta})\end{bmatrix}'=\begin{bmatrix}u_1 & u_2 & u_3\end{bmatrix}'\tag{6}$$

As one can notice, the unknown parameters have been added to the enlarged state vector $\mathbf{x}$, thus there are six states in total. Two of the states correspond also to the output (position and speed). Moreover, the input vector (6) has been enlarged: the friction force has already been identified by a

pendulum experiment with the exoskeleton (with and without the weight of the arm). Measuring the angular velocity, the friction force can be treated as a known system input, reducing the state vector of the unknown parameters. As a result, there are four parameters that need to be identified online. Applying forward Euler discretization with the sampling period Δt the model becomes:

$$\mathbf{x}(k+1) = \mathbf{f}(\mathbf{x}(k),\mathbf{u}(k)) + \boldsymbol{\eta}_{\mathbf{x}}(k) \tag{7}$$

$$\mathbf{y}(k) = \mathbf{c}\mathbf{x}(k) + \boldsymbol{\eta}_{\mathbf{y}}(k) \tag{8}$$

where $\boldsymbol{\eta}_{\mathbf{x}}(k)$ is a vector of white noise affecting the state and $\boldsymbol{\eta}_{\mathbf{y}}(k)$ is a vector of the white noise affecting the outputs. Moreover:

$$\mathbf{f}(\mathbf{x}(k),\mathbf{u}(k)) = \begin{cases} x_1(k+1) = x_1(k) + x_2(k)\Delta t + \eta_{x_1}(k) \\ x_2(k+1) = \mathrm{f}_2(\mathbf{x}(k),\mathbf{u}(k)) + \eta_{x_2}(k) \\ x_3(k+1) = x_3(k) + \eta_{x_3}(k) \\ x_4(k+1) = x_4(k) + \eta_{x_4}(k) \\ x_5(k+1) = x_5(k) + \eta_{x_5}(k) \\ x_6(k+1) = x_6(k) + \eta_{x_6}(k) \end{cases} \tag{9}$$

$$\begin{aligned} \mathrm{f}_2(\mathbf{x}(k),\mathbf{u}(k)) = x_2(k) - \big(&\big(x_6(k) + x_3(k)u_1(k) + \cdots \\ &+ x_4(k)u_2(k)\big)x_1 - x_5(k)x_2(k) + \cdots \\ &+ \theta_{max_1}x_3(k)u_1(k) + \cdots \\ &+ \theta_{max_2}x_4(k)u_2(k) - u_3(k)\big)\Delta t \end{aligned} \tag{10}$$

$$\mathbf{c} = \begin{bmatrix} 1 & 0 & 0 & 0 & 0 & 0 & 0 \\ 0 & 1 & 0 & 0 & 0 & 0 & 0 \end{bmatrix} \tag{11}$$

The structure of the EKF is the following:

$$\begin{cases} \hat{\mathbf{x}}(k+1) = \mathbf{f}(\hat{\mathbf{x}}(k),\mathbf{u}(k)) + \mathbf{L}(k)\mathbf{e}(k) \\ \hat{\mathbf{y}}(k) = \mathbf{c}\hat{\mathbf{x}}(k) \\ \mathbf{e}(k) = \mathbf{y}(k) - \hat{\mathbf{y}}(k) \end{cases} \tag{12}$$

As one can see, the filter in (12) is based on the non-linear equation (7) and the filter gain $\mathbf{L}(k)$ is calculated from the Differential Riccati Equation (DRE). In order to calculate the DRE it is necessary to linearize (7) and to calculate the Jacobian matrix $\hat{\mathbf{F}}(k)$

$$\hat{\mathbf{F}}(k) = \left.\frac{\partial \mathbf{f}\big(\mathbf{x}(k),\mathbf{u}(k)\big)}{\partial \mathbf{x}(k)}\right|_{\mathbf{x}(k)=\hat{\mathbf{x}}(k|k-1)} \tag{13}$$

$$= \begin{bmatrix} 1 & \Delta t & 0 & 0 & 0 & 0 \\ \hat{\mathrm{f}}_{21} & \hat{\mathrm{f}}_{22} & \hat{\mathrm{f}}_{23} & \hat{\mathrm{f}}_{24} & \hat{\mathrm{f}}_{25} & \hat{\mathrm{f}}_{26} \\ 0 & 0 & 1 & 0 & 0 & 0 \\ 0 & 0 & 0 & 1 & 0 & 0 \\ 0 & 0 & 0 & 0 & 1 & 0 \\ 0 & 0 & 0 & 0 & 0 & 1 \end{bmatrix} \tag{14}$$

with

$$\begin{aligned} \hat{\mathrm{f}}_{21}\big(\hat{\mathbf{x}}(k|k-1),\mathbf{u}(k)\big) &= -\Delta t(\hat{x}_6 + \hat{x}_3u_1 + \hat{x}_4u_2) \\ \hat{\mathrm{f}}_{22}\big(\hat{\mathbf{x}}(k|k-1),\mathbf{u}(k)\big) &= 1 - \hat{x}_5\Delta t \\ \hat{\mathrm{f}}_{23}\big(\hat{\mathbf{x}}(k|k-1),\mathbf{u}(k)\big) &= (-u_1\hat{x}_1 + \theta_{max_1}u_1)\Delta t \\ \hat{\mathrm{f}}_{24}\big(\hat{\mathbf{x}}(k|k-1),\mathbf{u}(k)\big) &= (-u_2\hat{x}_1 + \theta_{max_2}u_2)\Delta t \\ \hat{\mathrm{f}}_{25}\big(\hat{\mathbf{x}}(k|k-1),\mathbf{u}(k)\big) &= -\hat{x}_2\Delta t \\ \hat{\mathrm{f}}_{26}\big(\hat{\mathbf{x}}(k|k-1),\mathbf{u}(k)\big) &= -\hat{x}_1\Delta t \end{aligned} \tag{15}$$

With the Jacobian matrix $\hat{\mathbf{F}}(k)$ it is possible to calculate the DRE and to reiterate for each step k the calculation of $\mathbf{P}(k+1)$, where

$$\begin{aligned} \mathbf{P}(k+1) = &\hat{\mathbf{F}}(k)\mathbf{P}(k)\hat{\mathbf{F}}(k)' + \mathbf{V}_1 + \cdots \\ &- \mathbf{L}(k)(\hat{\mathbf{F}}(k)\mathbf{P}(k)\hat{\mathbf{c}}(k)' + \mathbf{V}_{12})' \end{aligned} \tag{16}$$

$$\begin{aligned} \mathbf{L}(k) = &(\hat{\mathbf{F}}(k)\mathbf{P}(k)\hat{\mathbf{c}}(k)' + \mathbf{V}_{12})\cdot \\ &\cdot(\hat{\mathbf{c}}(k)\mathbf{P}(k)\hat{\mathbf{c}}(k)' + \mathbf{V}_2)^{-1} \end{aligned} \tag{17}$$

$\mathbf{V}_1$, $\mathbf{V}_2$ are respectively the covariance matrices of the noise that affect the state and the output. $\mathbf{V}_{12}$ is the covariance matrix between the noise of the state and the output. These covariance matrices are tuning parameters that can be properly selected in order to vary the performance of the filter. $\mathbf{V}_{12}$ is suppose to be equal to $\mathbf{0}$ (i.e. there is no correlation between the noises that affect the state and the outputs). For the measured outputs, the variance of the noise that affects the angular velocity is calculated from the data sets collected. On the other hand, as already explained in III-A, because of friction non-linearity, the tracking of the angular velocity is weighted more than the angular position: thus, for $\mathbf{V}_2$, the variance of the noise affecting the position is supposed to be very high. $\mathbf{V}_1$ has been tuned with an iterative process in order to reach the good identification performance in terms of speed of convergence and noise rejection. $\mathbf{P}(1)$, i.e. the initial value of the covariance prediction error, has been tuned very high, i.e. initial guess of the parameters values are supposed to be considerably different with respect to their real value.

B. Simulation results

The EKF described in subsection IV-A is firstly tested in simulation, using as real plant the model presented in subsection III-C with the parameters shown in Table II(a). The reference test is a step test, similar to the identification data set. White noises have been added to the input and the output in order to replicate the nature of the collected data. The simulation results has been analyzed in terms of:

- Normalized squared L2-norm of the angular velocity (and position) tracking error.
- Percentage error between parameters used for simulation and identified parameters.

The performance index $J_{L_2{}^2}(\hat{\theta})$ is equal to 0.08% while $J_{L_2{}^2}(\hat{\theta})$ is equal to 0.1%. The EKF is able to perfectly track angular velocity and position. The comparison between simulation parameters and the estimated ones can be seen in Fig. 9. The time for convergence (i.e. for reaching the $\pm 10\%$ range with respect to the simulation values) is less then 10 seconds in the worst case ($\tilde{K}_1$). The percentage estimation error is calculated based on the average value of the parameter estimate after the convergence. Table III shows that the estimated values are very closed to the ones ones used in the simulation model.

C. Experimental results

EKF has been also applied on real experimental data, starting from the data collected for identification (see Fig. 4).

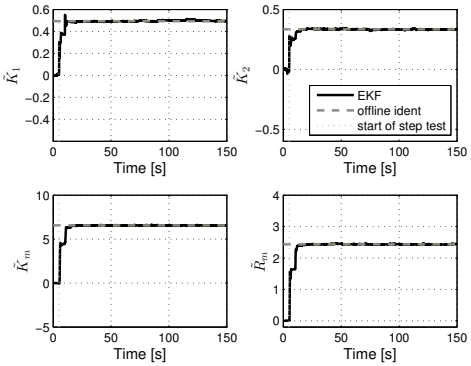

Fig. 9 - Results for EKF in simulation. The figures show the comparison between simulation and estimated parameters.

TABLE III

PERCENTAGE ESTIMATION ERROR OF ONLINE IDENTIFICATION IN SIMULATION.

Estimated Parameter	Error [%]
$\tilde{K}_1$	0.64
$\tilde{K}_2$	-0.02
$\tilde{K}_m$	-0.04
$\tilde{R}_m$	0.02

The normalized squared L2-norms, $J_{L_2{}^2}(\hat{\theta})$ is equal to 4.2% while $J_{L_2{}^2}(\hat{\theta})$ is equal to 6.7%. As expected these values are significantly worse than the simulation ones. However the performance indices of the off-line identification are the real benchmark. The normalized squared L2-norm calculated for the EKF estimation is slightly better than the one shown in Table II(b) for the off-line identified model. Fig. 10

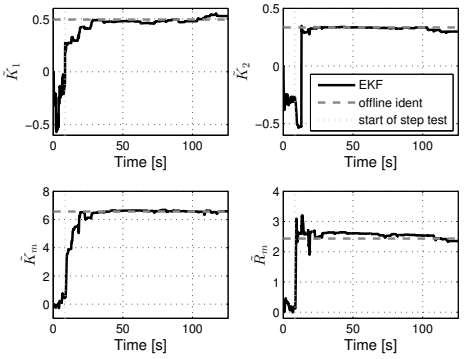

Fig. 10 - Results for EKF in simulation. The figures show the comparison between offline and online estimated parameters.

displays the comparison between online and offline identified parameters (cf. Table II(a)) using the same data set of Fig. 4. With respect to the simulation results, the average time for convergence is 15 seconds. For the worst case, i.e. $\tilde{K}_1$, it is 20 seconds. In Table IV it is possible to see that the values estimated by EKF differ by less than 5% from the offline estimated ones.

TABLE IV

PERCENTAGE DIFFERENCE OF OFFLINE AND ONLINE ESTIMATED PARAMETERS FOR THE EXPERIMENTAL DATA.

Estimated Parameter	Difference [%]
$\tilde{K}_1$	-0.57
$\tilde{K}_2$	-3.89
$\tilde{K}_m$	0.29
$\tilde{R}_m$	3.07

V. CONCLUSIONS

The model proposed in Section III-C is able to describe with a small set of parameters the horizontal shoulder abduction and adduction movement actuated by a pair of artificially stimulated antagonistic muscles. Starting from this model, model-based control strategies can be designed. The model parameters can be estimated offline or online from short experiments. The proposed extended Kalman filter for online identification possesses a fast convergence of less than 20 seconds. Moreover, the online estimation give the opportunity of designing an adaptive controller (self-tuning control) that changes its parameters in run-time. This is also very important to take into account other slow dynamics, such as the muscular fatigue. A validation of the proposed models and identification approaches with spinal cord injuries patients will be carried out in a next step. Future work involves also the design of such controllers in order to control horizontal shoulder abduction and adduction movement.

REFERENCES

[1] R. Riener, "Model-based development of neuroprostheses for paraplegic patients," in *Philosophical Transactions of the Royal Society of London. Series B: Biological Science*, vol. 354, pp. 877–894, May 1999.

[2] T. Schauer, N.-O. Negård, F. Previdi, K. Hunt, M. Fraser, E. Ferchland, and J. Raisch, "Online identification and nonlinear control of the electrically stimulated quadriceps muscle," *Control Engineering Practice*, vol. 13, no. 9, pp. 1207–1219, 2005.

[3] T. Schauer, K. Hunt, M. Faser, W. Stewart, and F. Previdi, "Sliding-mode control of knee-joint angle: Experimental results," in *Proceedings of IFESS*, 2002.

[4] F. Previdi, "Identification of black-box nonlinear models for lower limb movement control using functional electrical stimulation," *Control Engineering Practice*, pp. 91–99, 2002.

[5] D. A. Winter, *Biomechanics and Motor Control of Human Movement*, ch. Muscle Mechanics. John Wiley & Sons, Inc., fourth edition ed., 2009.

[6] A. V. Hill, "First and last experiments in muscle mechanics," *Cambridge University Press*, 1970.

[7] C. Klauer, J. Raisch, and T. Schauer, "Linearisation of electrically stimulated muscles by feedback control of the muscular recruitment measured by evoked EMG ," in *Proc. of MMAR*, pp. 108–113, IEEE, 2012.

[8] A. V. Hill, "The heat of shortening and dynamic constants of muscle," in *Proceedings of Royal Society B*, pp. 136–195, 1938.

[9] R. Riener and T. Fuhr, "Patient-driven control of FES-supported standing up," *IEEE Trans. Rehabil. Eng*, vol. 6, no. 2, pp. 113–124, 1998.

[10] D. Bennett, J. Hollerbach, Y. Xu, and I. Hunter, "Time-varying stiffness of human elbow joint during cyclic voluntary movement," *Experimental Brain Research*, vol. 88, pp. 433–442, 1992.

[11] R. R. Carter, P. E. Crago, and P. H. Gorman, "Nonlinear stretch reflex interaction during cocontraction," *Journal of Neurophysiology*, no. 69, pp. 943–952, 1993.

[12] R. E. Kearney and I. W. Hunter, "System identification of human joint dynamics," *Critical reviews in biomedical engineering*, no. 18, pp. 55–87, 1990.